Fish and Shellfish Immunology 89 (2019) 411–419

Contents lists available at ScienceDirect

Fish and Shellfish Immunology

journal homepage: www.elsevier.com/locate/fsi

Full length article

Functional characterization of dark sleeper (*Odontobutis obscura*) IRF3 in IFN regulation

Zhuocong Li[a,c,1], Jian Chen[b,1], Pei Li[b], Xi-yin Li[c], Longfeng Lu[c], Shun Li[c,*]

[a] University of Chinese Academy of Sciences, Beijing, China
[b] Fisheries Research Institute, Wuhan Academy of Agricultural Sciences, Wuhan, China
[c] State Key Laboratory of Freshwater Ecology and Biotechnology, Institute of Hydrobiology, Chinese Academy of Sciences, Wuhan, China

ARTICLE INFO

Keywords:
IRF3
IFN
RLRs
Odontobutis obscura

ABSTRACT

The dark sleeper, *Odontobutis obscura* (*O. obscura*), is a commercially important species of freshwater sleeper native to East Asia. However, its molecular biology system is unexplored, including the interferon (IFN) signaling pathway, which is crucial to the antiviral response. In this study, we characterised the IFN regulation pattern of dark sleeper interferon regulatory factor 3 (OdIRF3), supplementing evidence of the conservation of this classical pathway in fish. First, the open reading frame (ORF) of OdIRF3 was cloned from the liver tissue by Rapid amplification of cDNA ends (RACE). Amino acid sequence analysis suggested that OdIRF3 is homologous with other fish IRF3 and that the N-terminal DNA-binding domain (DBD) and the C-terminal IRF-association domain (IAD) are conserved. Then, the cellular distribution demonstrated that OdIRF3 is located in the cytoplasm region and transfers into the nuclear region under stimulation. For the function identification, OdIRF3 activated several types of IFN promoters and induced downstream interferon stimulated genes (ISGs) expression. Finally, the overexpression of OdIRF3 significantly decreased viral proliferation. Taken together, these data systematically characterised the sequence, cellular location, and function in IFN expression of OdIRF3, shedding light on the molecular biology mechanism of the dark sleeper.

1. Introduction

Pattern recognition receptors (PRRs) recognize pathogens and, subsequently, activate signaling pathways to promote interferon (IFN) production [1,2]. Interferon regulatory factors (IRFs) are crucial transcription factors that initiate IFN activation. Most IRFs contain an N-terminal DNA-binding domain (DBD) that mediates an interaction with the target gene promoters and a C-terminal IRF-association domain (IAD) that associates with other proteins. In recent years, great progress has been made in identifying fish IRFs involved in the IFN antiviral response, with 11 IRF members having been identified (IRF1a and IRF1b make up IRF1) [3]. Zebrafish (*Danio rerio*) IRF1 (DrIRF1) is a positive regulator of fish IFN in the antiviral response. The overexpression of DrIRF1 induces IFN and IFN-stimulated gene activation, hence protecting epithelioma papulosum cyprinid (EPC) cells against spring viremia carp virus (SVCV) infection [4]. Grass carp (*Ctenopharyngodon idella*) IRF2 (CiIRF2) binds to promoters such as CiIFN, CiPKR, and CiPKZ with high affinity by means of its DBD, and downregulates the transcription activity of these genes [5]. Zebrafish IRF6 (DrIRF6) is a positive regulator of IFN transcription that can be phosphorylated by both MyD88 and TBK1, and activates the transcription of interferon stimulated genes (ISGs) of host cells [6]. Barbel chub (*Squaliobarbus curriculus*) IRF7 (ScIRF7) induces the upregulation of IFN after grass carp reovirus (GCRV) infection [7]. Zebrafish IRF9 (DrIRF9) promoter can be activated by the combination of IRF9 and STAT2. In addition, both recombinant crucian carp (*Carassius auratus* L.) IFN protein and the overexpression of zebrafish IFNγ2 led to a significant increase in the crucian carp IRF9 protein in cells [8]. Lastly, zebrafish IRF10 (DrIRF10) inhibits the activation of zebrafish IFNφ1 (DrIFNφ1) and DrIFNφ3 promoters in EPC cells in the presence of polyinosinic:polycytidylic acid (poly (I:C)) stimulation, which acts as a negative regulator of the IFN response [9].

In mammals, IRF3 is a key transcription factor involved in RLR/TLR signaling pathways. Phosphorylated IRF3 forms dimers, and it is transferred from the cytoplasm to the nuclei where it binds to interferon-sensitive response element (ISRE) motifs to initiate the transcription of target genes, including IFN and other ISGs [10]. In fish, a lot of research has been conducted on IRF3 from a number of different

* Corresponding author. Institute of Hydrobiology, Chinese Academy of Sciences, 7 Donghu South Road, Wuhan, Hubei, 430072, China.
E-mail address: bob@ihb.ac.cn (S. Li).
[1] These authors contributed to the work equally.

https://doi.org/10.1016/j.fsi.2019.04.019
Received 19 October 2018; Received in revised form 29 March 2019; Accepted 5 April 2019
Available online 10 April 2019
1050-4648/

species. In mandarin fish, consistent with mammals, IRF3 aggregates in the nucleus after phosphorylation and increases the transcriptional activity of the IFN promoter, playing a critical role in defense against viral infection [11]. Different to what has been shown in mammals, CaIRF3 is significantly upregulated by IFN, but also shows significant sequence differences to its mammalian ortholog [12]. Studies of ScIRF3 found that type I IFN is significantly positively correlated with ScIRF3 in the intestine. In addition, it was found that GCRV titer is significantly decreased in GCRV-infected ScIRF3-overexpressing cells [13]. Lastly, DrIRF3 activates DrIFNφ1 rather than DrIFNφ3, and facilitates the binding of DrIRF1 and DrIRF7 to the promoters of DrIFNφ1 and DrIFNφ3, respectively. Interestingly, DrIRF3 has dual effects on DrIRF1-mediated DrIFNφ3 gene expression, having an inhibitory effect at lower concentrations and synergistic effects at higher concentrations [14].

In this study, we report the characterization of dark sleeper (*Odontobutis obscura*) IRF3 (OdIRF3). Our findings demonstrate that OdIRF3 is active on the IFN promoters of both in zebrafish and grass carp cells and significantly induces ISG expression. Overall, it is shown that OdIRF3 plays a critical role in the antiviral immune response of this fish as a positive IFN regulator.

2. Materials and methods

2.1. Cells and viruses

Epithelioma papulosum cyprinid (EPC) (ATCC number: CLR-2872) and Grass carp ovary (GCO) cells were purchased from China Center For Type Culture Collection [15]. EPC and GCO cells were maintained at 28 °C in 5.0% CO_2 in medium 199 (Invitrogen) supplemented with 10% fetal bovine serum (FBS, Invitrogen). HEK 293T (ATCC number: CRL-3216) cells were grown at 37 °C in 5.0% CO_2 in DMEM medium (Invitrogen) supplemented with 10% FBS. Spring viremia of carp virus (SVCV) was propagated in EPC cells until cytopathic effects (CPE) were observed, then the cultured media with cells was harvested and stored at −80 °C until needed.

2.2. Homologous cloning of the OdIRF3 gene

To identify IRF3 cDNA sequence from dark sleeper, degenerate primers were designed based on the multiple alignments of the predicted IRF3 sequences in *Larimichthys crocea* (accession No., JQ249912.1), *Paralichthys olivaceus* (accession No., GU017417.1), and *Oplegnathus fasciatus* (accession No., KF267453.1) and the predicted IRF3 sequence in *Takifugu rubripes* (accession No., XM_003961282.2). The degenerate PCR amplification for a partial fragment of IRF3 was demonstrated using the dark sleeper spleen cDNA according to the following PCR condition: 1 cycle of 95 °C/5 min; 35 cycles of 95 °C/30 s, 50 °C/30 s, 72 °C/2 min; 1 cycle of 72 °C/10 min. Amplified PCR products were ligated into pMD™18-T Vector, transformed into the competent *Escherichia coli* TOP10 cells, and plated on the LB-agar petri-dish. Positive colonies containing expected size insert were screened by colony PCR (*Escherichia coli* cells from a colony were picked up from agar plates by using a sterile pipette tip and resuspended into 10 μl distilled water, the mixture was vortexed and subjected to PCR analysis). Four of them were picked up and sent to a commercial company (Wuhan TSINGKE Biological Technology, China) for sequencing.

2.3. Cloning the full-length OdIRF3 cDNA and plasmid construction

Rapid amplification of cDNA ends (RACE) was carried out using the 5′ RACE system (Invitrogen) and BD SMART™ RACE cDNA amplification kit (BD Biosciences Clontech) according to the manufacturer's instruction. The first strand cDNA synthesis and RACE were performed on spleen-derived RNA. To obtain the 3′ unknown region, primer pairs OdI3F3a/APT and OdI3F4a/AP (Table 1), were used for the primary PCR and the nested PCR respectively. The amplified PCR product was cloned and sequenced as described above. Similarly, the 5′ end of OdIRF3 was obtained by nested PCR using primer pairs OdI3F5a/APG and OdI3F6a/AP (Table 1). The full-length cDNA sequence was confirmed by sequencing the PCR product amplified by primers OdI3FP and OdI3RP (Table 1) within the predicted 5 and 3 untranslated regions respectively. The open reading frame (ORF) of OdIRF3 was subcloned into pcDNA3.1 (+) (Invitrogen) and pCMV-Myc (Clontech) respectively. For subcellular localization, the ORF of OdIRF3 was inserted into pEGFP-N3 vector (Clontech). The plasmids containing IFNφ1pro-Luc (NM_207640.1), IFNφ3pro-Luc (NM_001111083.1), EPCIFN, gcIFN1, and ISRE-Luc in pGL3-Basic luciferase reporter vectors (Promega) were constructed as previously described [16]. All constructs were confirmed by DNA sequencing.

2.4. Sequence alignment and phylogenetic analysis

Sequence homology was obtained using BLAST program (http://www.ncbi.nlm.nih.gov/blast). The deduced amino acid sequence was analyzed with the Expert Protein Analysis System (http://www.expasy.org/). The protein domains were predicted by Simple Modular Architecture Research Tool (SMART) (http://smart.embl-heidelberg.de/). Phylogenetic and molecular evolutionary analyses were conducted using the GeneDoc following the alignment of amino acid sequences. Comparisons of the predicted domains, motifs and features of IRF3 from different species were performed on the Molecular Evolutionary Genetics Analysis (MEGA) software version 4.1. The phylogenetic tree was constructed using the Neighbor-joining method (NJ) within the MEGA7 program which was bootstrapped 500 times. All gene sequences used within this study were derived from GenBank.

2.5. Luciferase activity assay

EPC cells were seeded into 24-well plates overnight and co-transfected with 0.25 μg luciferase reporter plasmid (IFNφ1pro-Luc, IFNφ3pro-Luc, ISRE-Luc or EPCIFN-Luc), 0.05 μg of Renilla luciferase internal control vector (pRL-TK, Promega) and 0.5 μg pCMV-Myc-OdIRF3. Empty vector pCMV-Myc was used to maintain equivalent amounts of DNA in each well. GCO cells were used to detect ISRE-Luc and gcIFN1-Luc. At 24 h post-transfection, the cells were washed with PBS and lysed for measuring luciferase activity using the Dual-Luciferase Reporter Assay System, according to the manufacturer's instructions (Promega). The results for each experiment were representative of more than three independent experiments, each performed in triplicate.

2.6. Fluorescent microscopy

EPC cells were plated onto coverslips in 6-well plates and transfected with 3 μg EGFP-OdIRF3 or EGFP-N3 (control). After 24 h, the cells were untreated (null) or transfected with 2 μg poly (I:C) for 12 h. Following this, the cells were washed twice with PBS and fixed with 4% paraformaldehyde (PFA) for 1 h. After draining the fixative, the cells were stained with DAPI (1 μg/ml; Beyotime) for 30 min in a dark at room temperature. Finally, the coverslips were washed and observed using a confocal microscope under a × 63 oil immersion objective (SP8; Leica Microsystems).

2.7. RNA extraction, reverse transcription, and quantitative real-time PCR (qPCR)

For constitutive expression, total RNA was extracted from brain, pituitarium, eye, gill, heart, liver, muscle, spleen, head kidney, and ovary from three apparently healthy dark sleepers. Total RNAs of EPC cells or tissues were extracted by the Trizol reagent (Invitrogen). First-strand cDNA was synthesized by using a GoScript Reverse Transcription

Table 1
Primers used in this study.

Name	Sequences (5' →3')	Purpose
OdI3F1a	GGCAACAGSAGTATCCAGTAAYG	RACE
OdI3F2a	CRTTACTGGATACTSCTGTTGCC	
OdI3F3a	GCTATATCTACCTCCCACAAG	
OdI3F4a	GATGTGATTGGAGGACATGTG	
APT	CCAGACTCGTGGCTGATGCATTTTTTTTTTTTTTTTTTV	
APG	CCAGACTCGTGGCTGATGCAGGGGGGGGGGGGGGGGV	
AP	CCAGACTCGTGGCTGATGCA	
OdI3F5a	CTTGTGGGAGGTAGATATAGC	
OdI3F6a	ACATGGCTGGCTCTCTTGTG	
OdI3FP	ATGTCTCACTCCAGACCTC	Eukaryotic expression
OdI3RP	TYAGYACAKYTCCATCATCTC	
M13F	TGTAAAACGACGGCCAGT	Colony PCR
M13R	CAGGAAACAGCTATGACC	
qPCR-OdIRF3-FP	CTACACAAGAGAGCCAGC	Real-time PCR
qPCR-OdIRF3-RP	TCAGGGCCAATATTCAGC	
qPCR—IFN—EPC-FP	ATGAAAACTCAAATGTGGACGTA	
qPCR—IFN—EPC-RP	GATAGTTTCCACCCATTTCCTTAA	
qPCR-VIG1-EPC-FP	AGCGAGGCTTACGACTTCTG	
qPCR-VIG1-EPC-RP	GCACCAACTCTCCCAGAAAA	
qPCR-MAVS-EPC-FP	GAATGTCCCTGTCCGAGAAA	
qPCR-MAVS-EPC-RP	TCTGAACATGCTCGTTTGCAG	
qPCR-β-Actin-FP	CACTGTGCCCATCTACGAG	
qPCR-β-Actin-RP	CCATCTCCTGCTCGAAGTC	
qPCR-Od-β-actin1-FP	CTCTTCCAGCCATCCTTCCT	
qPCR-Od-β-actin1-RP	TCAGGTGGGGCAATGATCTT	

System (Promega) according to the manufacturer's instructions. qPCR was performed with Fast SYBR Green master mix (BioRad) on the CFX96 Real-Time System (BioRad). PCR conditions were as follows: 95 °C for 5 min, then 40 cycles of 95 °C for 20 s, 60 °C for 20 s, 72 °C for 20 s and the cyprinid β-actin primers were used to normalise the data. The primer sequences are shown in Table 1. The specificity of the PCR amplification for all primer sets was verified from the dissociation curves. The identity of each PCR products was confirmed by dideoxy-mediated chain termination sequencing at Wuhan TSINGKE Biological Technology Inc. The relative fold changes were calculated using the $2^{-\Delta\Delta Ct}$ method [17]. Three independent experiments were conducted for statistical analysis.

2.8. Transient transfection and virus infection

Transient transfections were performed in EPC cells seeded in 6-well or 24-well plates by using X-tremeGENE HP DNA Transfection Reagent (Roche) according to the manufacturer's protocol. For the antiviral assay using 24-well plates, EPC cells were transfected with 0.5 μg pCMV-Myc-OdIRF3 or the empty vector. At 24 h post-transfection, cells were infected with SVCV at a multiplicity of infection (MOI = 100). After 2 or 3 d, supernatant aliquots were harvested for detection of virus titers, the cell monolayers were fixed by 4% paraformaldehyde (PFA) and stained with 1% crystal violet for visualizing CPE. For virus titration, 200 μl of culture medium were collected at 48 h post-infection, and used for plaque assay. The supernatants were subjected to 3-fold serial dilutions and then added (100 μl) onto a monolayer of EPC cells cultured in a 96-well plate. After 48 or 72 h, the medium was removed and the cells were washed with PBS, fixed by 4% PFA and stained with 1% crystal violet. The virus titer was expressed as 50% tissue culture infective dose ($TCID_{50}$/ml). Results are representative of three independent experiments.

2.9. Statistics analysis

The results are expressed as mean ± SEM. Data were analyzed using a Student's unpaired *t*-tests. A p value < 0.05 was considered to be statistically significant.

3. Results

3.1. Molecular cloning and phylogenetic analysis of IRF3

Initially, the coding sequence (CDS) of OdIRF3 was characterised and found to be composed of 1383 nucleotides, predicted to code for 460 amino acid residues. A multiple alignment was used to investigate the homology of OdIRF3 with previously characterised genes. This showed, good conservation was found around the N-terminal DBD (8–104) and C-terminal IAD (258–436) (Fig. 1), indicating that its function could be similar to that found with other fish IRF3. Phylogenetic analyses of OdIRF3 with previously characterised IRF3 members from several species clearly demonstrated its close relationship to other fish, in particular *Siniperca chuatsi*, *Lateolabrax japonicus* and *Trachinotus ovatus* (Fig. 2).

3.2. Tissue expression pattern of OdIRF3 in healthy fish

As IRF3 is a pivotal and extensive transcription factor for hosts, the tissue distribution pattern of OdIRF3 was monitored by qRT-PCR. In this experiment, ten different tissues (Brain, Pituitarium, Eye, Gill, Heart, Liver, Muscle, Spleen, Head Kidney, Ovary) of three dark sleepers were chosen for analysis. As illustrated, the transcripts of OdIRF3 were founded to be constitutively expressed in all the selected tissues, with the highest level observed in the pituitary and the lowest level in the kidney tissue (Fig. 3). These results indicate that OdIRF3 was ubiquitously expressed in different tissues.

3.3. IFN and ISRE are activated by OdIRF3

Because IRF3 is a crucial factor in IFN activation, the function of OdIRF3 was investigated. DrIFNφ1 and DrIFNφ3 were co-transfected with OdIRF3 into EPCs, and the activities of these promoters were measured by luciferase reporter gene assays. These assays revealed that OdIRF3 significantly upregulated the activity of the DrIFNφ1 promoter,

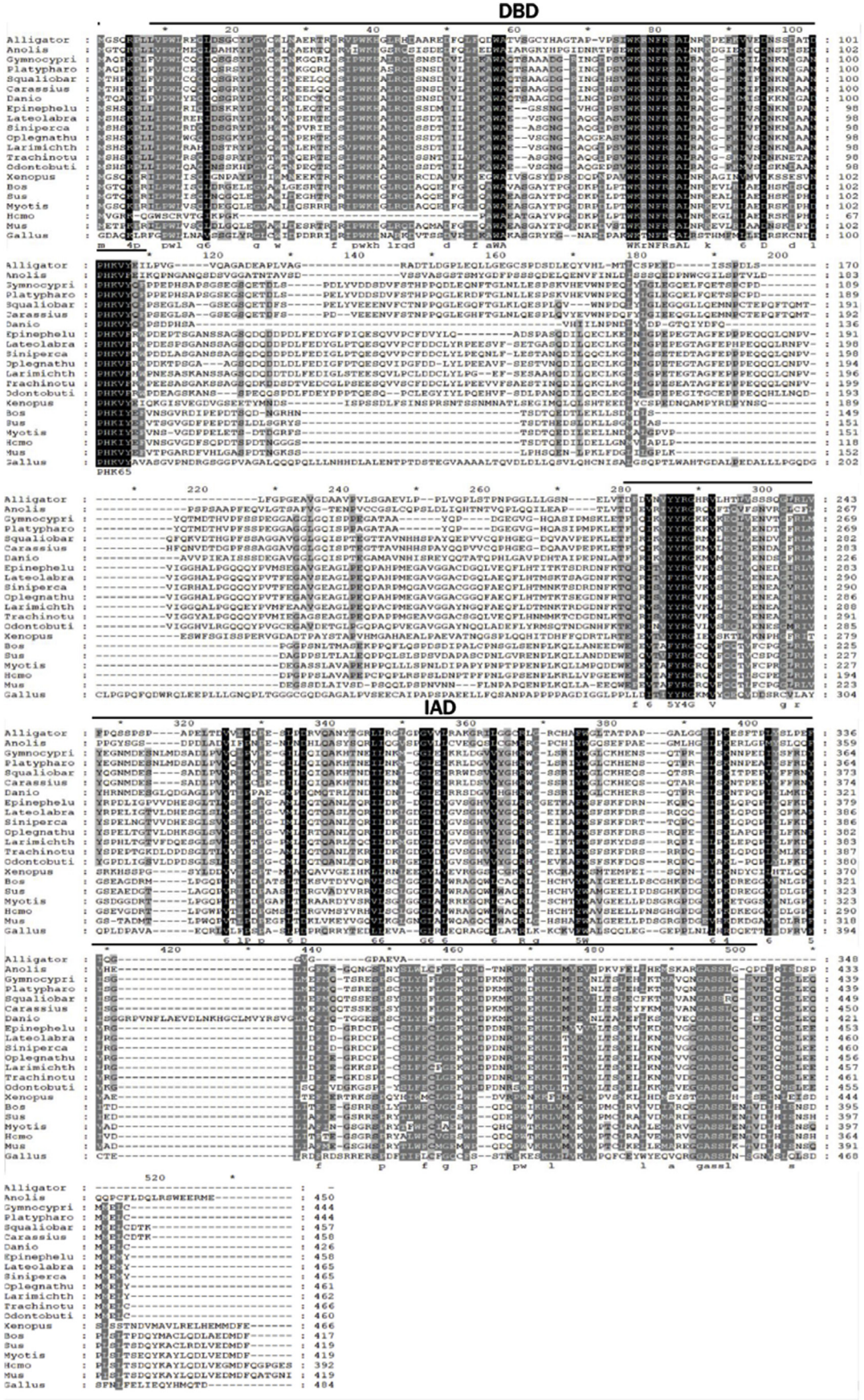

(caption on next page)

Fig. 1. Multiple alignment of the amino acid sequence of OdIRF3 homologue with IRF3 sequences from vertebrates using GeneDoc. Conserved DBD was showed in the black box, IAD was showed in the gray box. The GenBank numbers of the sequences are as follows: *Odontobutis obscura* (dark sleeper), MK433209; *Alligator sinensis* PREDICTED (Chinese alligator), XP_025051910.1; *Anolis carolinensis* (anole), AJG44477.1; Gymnocypris przewalskii, AUL77382.1; *Platypharodon extremus*, AUL77375.1; *Squaliobarbus curriculus* (brown trout), AQV11930.1; *Carassius auratus* (goldfish), ADO52204.1; *Danio rerio* (zebrafish), NP_001137376.1; *Epinephelus coioides* (grouper), AGC31487.1; *Lateolabrax japonicus* (black spotfed bass), AXI69832.1; *Siniperca chuatsi* (mandarin fish), AVC70699.1; *Oplegnathus fasciatus* (Stone bream), AHX37215.1; *Larimichthys crocea* (large yellow croaker), NP_001290316.1; *Trachinotus ovatus* (golden pomfret), AWY04222.1; *Xenopus laevis* (frog), NP_001079588.1; *Bos taurus* (cattle), NP_001025016.1; *Sus scrofa* (wild boar), ADU85980.1; *Myotis davidii* (large mouse-eared bat), AOQ26355.1; *Homo sapiens* (human), NP_001184052.1; *Mus musculus* (mouse), NP_058545.1; *Gallus* (chicken), NP_990703.1.

compared to the control group, by 42-fold (Fig. 4A). In contrast, the expression level of DrIFNφ3 showed no significant change (Fig. 4B). ISRE-Luc was used to monitor IFN signaling, which after transfection of the EPC cells with OdIRF3 and ISRE-Luc, enhanced the activity of the ISRE promoter by 3.1-fold (Fig. 4C). The activity of the EPC IFN promoter was also measured and showed significant upregulation by 8.8-fold, compared to the control group (Fig. 4D). Lastly, ISRE or GcIFN1 were co-transfected with OdIRF3 into GCO cells, with both being significantly activated by OdIRF3. The expression levels of GcIFN1 and ISRE were increased by 3.7-fold and 4.5-fold compared with the control group, respectively (Fig. 4E and F). These results indicate that OdIRF3 can activate promoters involved in the IFN signaling pathway.

3.4. Cytoplasm localization of OdIRF3

To determine the cellular location of OdIRF3, confocal microscopy analysis was used to investigate the subcellular localization of OdIRF3 in the absence and presence of poly (I:C) stimulation (Fig. 5). Within the EPC cells containing the controls with or without poly (I:C) stimulation, the fluorescent signals were distributed in both the cytosol and nucleus. In cells containing OdIRF3 with no poly (I:C) stimulation, green signals were detected in the cytosol surrounding the nucleus (blue), while no detectable signals were seen within the nucleus. However, after poly (I:C) stimulation, the green fluorescent signals were also detected in the nucleus (Fig. 5). This suggests that OdIRF3 was only distributed in the cytosol in unstimulated cells and nuclear aggregation of OdIRF3 occurs after poly (I:C) stimulation.

3.5. ISG expression is induced by OdIRF3

To investigate the role of OdIRF3 in IFN transcript production, we transfected EPC cells with OdIRF3 and extracted total RNA (Fig. 6). qRT-PCR was employed to detect selected interferon-stimulated genes: epcifn, epcmavs, and epcvig1. The transcription levels of epcifn and epcmavs increased significantly compared to the control, indicating that OdIRF3 is capable of activating ISG transcription. The mRNA level of epcifn increased 33-fold and epcmavs increased 7.7-fold compared with the control group. In contrast, epcvig1 increased by 1.8-fold and

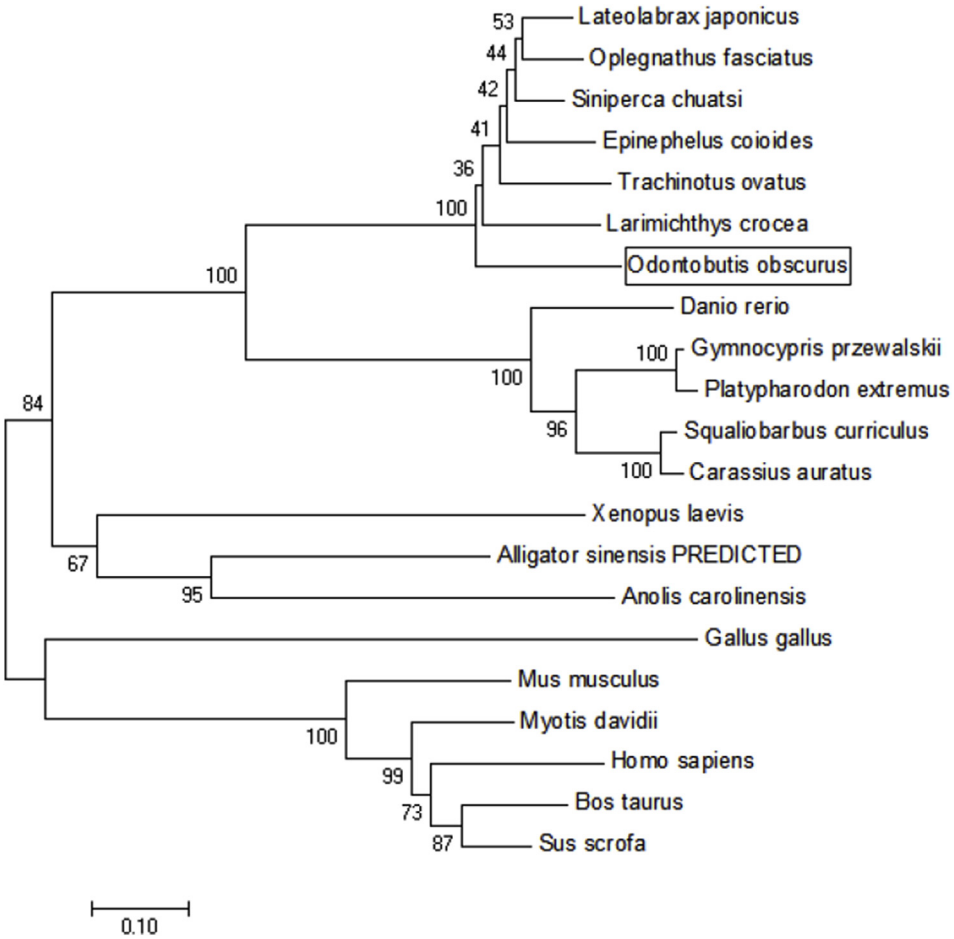

Fig. 2. Phylogenetic analysis of IRF3 homologues from different species. The rooted tree was constructed by the neighbor-joining method and was bootstrapped 500 times using MEGA 7.0 software. Numbers at the nodes indicate bootstrap values. The scale bar is 0.1.

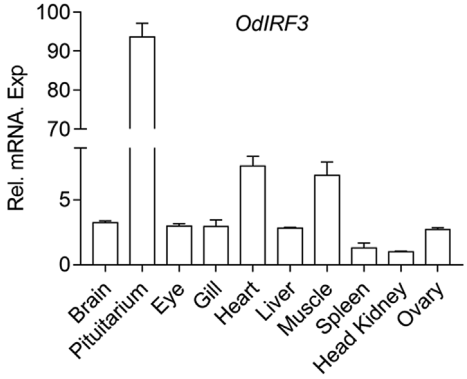

Fig. 3. Relative mRNA expression of OdIRF3 in different tissues. Total RNAs from different tissues of three dark sleepers were extracted to examine the transcripts of OdIRF3 and *β-actin* was used as an internal control for normalization to give relative expression. The expression levels in the other tissues are shown as fold induction compared with the head kidney (for which their relative expressions were set to 1). Error bars represents the means ± SEM (n = 3), and the experiments were repeated three time with similar results.

was not significant.

3.6. Overexpression of OdIRF3 induces a strong antiviral state in EPC cells

SVCV is an ssRNA virus and infects EPC cells efficiently. EPC cells were transfected with OdIRF3 and infected with SVCV to determine the role of OdIRF3 in the host immune response against viral infection. At 2 d post-infection, infection of EPC cells transfected with empty vector by SVCV led to a complete CPE. In contrast, transfection of these cells with OdIRF3 fully protected them against SVCV infection (Fig. 7A). Measurement of the viral titer showed that overexpression of OdIRF3 decreased the viral titer 19000-fold compared to that in control cells (Fig. 7B).

4. Discussion

The IRF family consists of integral transcription factors that function in regulation of IFN expression in defense against viral infection. Besides IFN modulation, they also play crucial roles in tumor formation, stress responses, development, and immune cell regulation [18,19]. Nine members of the IRFs have been identified in mammals. These conserved IRFs contain a DNA binding domain (DBD) at the N terminus and an IRF-association domain (IAD) at the C terminus, except for IRF1 and IRF2, which only possess the DBD [20]. Most IRFs are positive regulators of IFN expression, although there are negative IFN regulators such as IRF2 and IRF4. IRF2 activates a transcriptional repressor of IFN expression [21–23]; IRF4 balances antiviral responses in host cells through interaction with IRF5 [24]. In fish, 11 members of IRFs have been identified, of which two are homologues of IRF1. They were once called IRF1a and IRF1b, but have been renamed IRF1 and IRF11 [25]. To date, several studies have revealed the functional differences of IRFs between fish and mammals. As an example, IRF10, found in fish, exhibits negative regulation of IFN that is absent in mammals. In the current research, OdIRF3 positively modulated IFN expression, which is consistent with that in mammals, demonstrating that IRF3 is conserved in lower and higher vertebrates [26].

In this investigation, OdIRF3 had the highest expression in the pituitary, whereas it was relatively low in the spleen and head kidney. The pituitary plays an important role in various biological processes of fish, such as formation of the hypothalamus–pituitary–interrenal axis, which is associated with stress response, metabolism, and immune response [27,28]; thus the high level of OdIRF3 there may reflect its function.

There are two possibilities for the lower expression of OdIRF3 in the spleen and the head kidney: (1) OdIRF3 is not involved in adaptive immunity as are other IRFs such as IRF4 or IRF8. (2) mRNA expression checking was performed in healthy fish, in which irf3 is not necessary for up-regulation.

In our analysis, OdIRF3 exhibited a powerful effect on zebrafish and grass carp IFN promoter activation. OdIRF3 induced the expression of DrIFNφ1 but had no significant effect on the expression of DrIFNφ3, probably due to the signaling pathways of DrIFNφ1 and DrIFNφ3

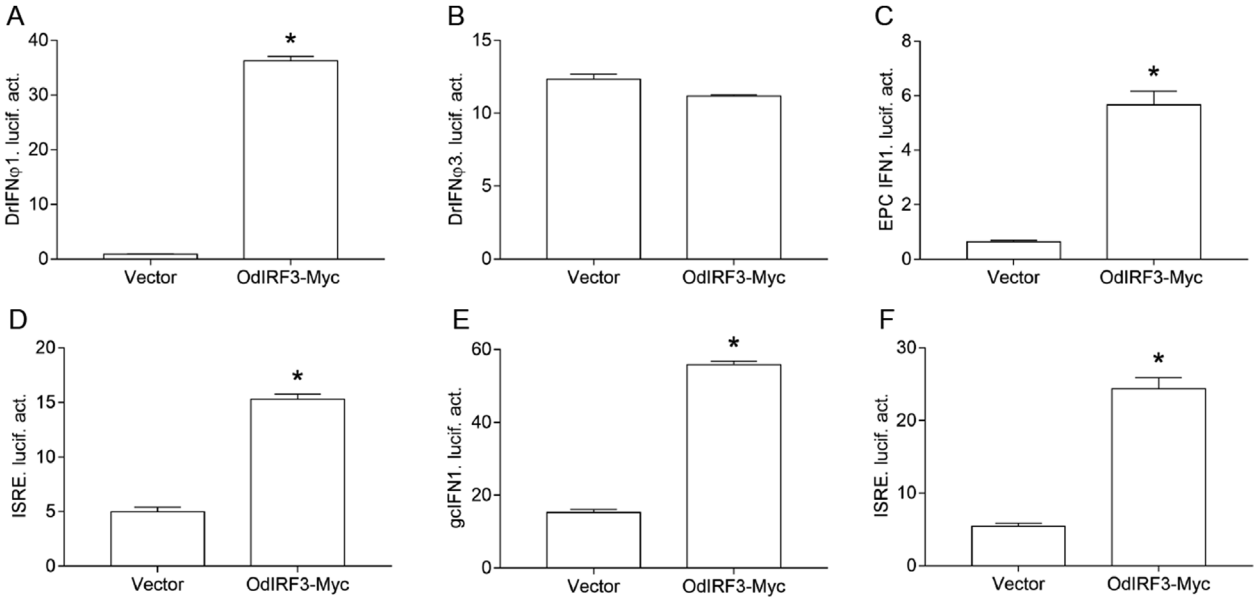

Fig. 4. Activation of DrIFNφ1, DrIFNφ3 and ISRE promoters by overexpression of OdIRF3 within EPCs. EPC cells were seeded in 24-well plates overnight and co-transfected with pCMV-Myc or OdIRF3-Myc and DrIFNφ1 pro-Luc (A), DrIFNφ3 pro-Luc (B), EPC IFN pro-Luc (C), ISRE-Luc (D). GCO cells were treated the same way and co-transfected with pCMV-Myc or OdIRF3-Myc and gcIFN1 pro-Luc (E), ISRE-Luc (F). The luciferase assays were performed 24 h after transfection. Error bars represents the means ± SEM (n = 3), and the experiments were repeated three time with similar results. Asterisks indicate significant differences from control (*$p < 0.05$).

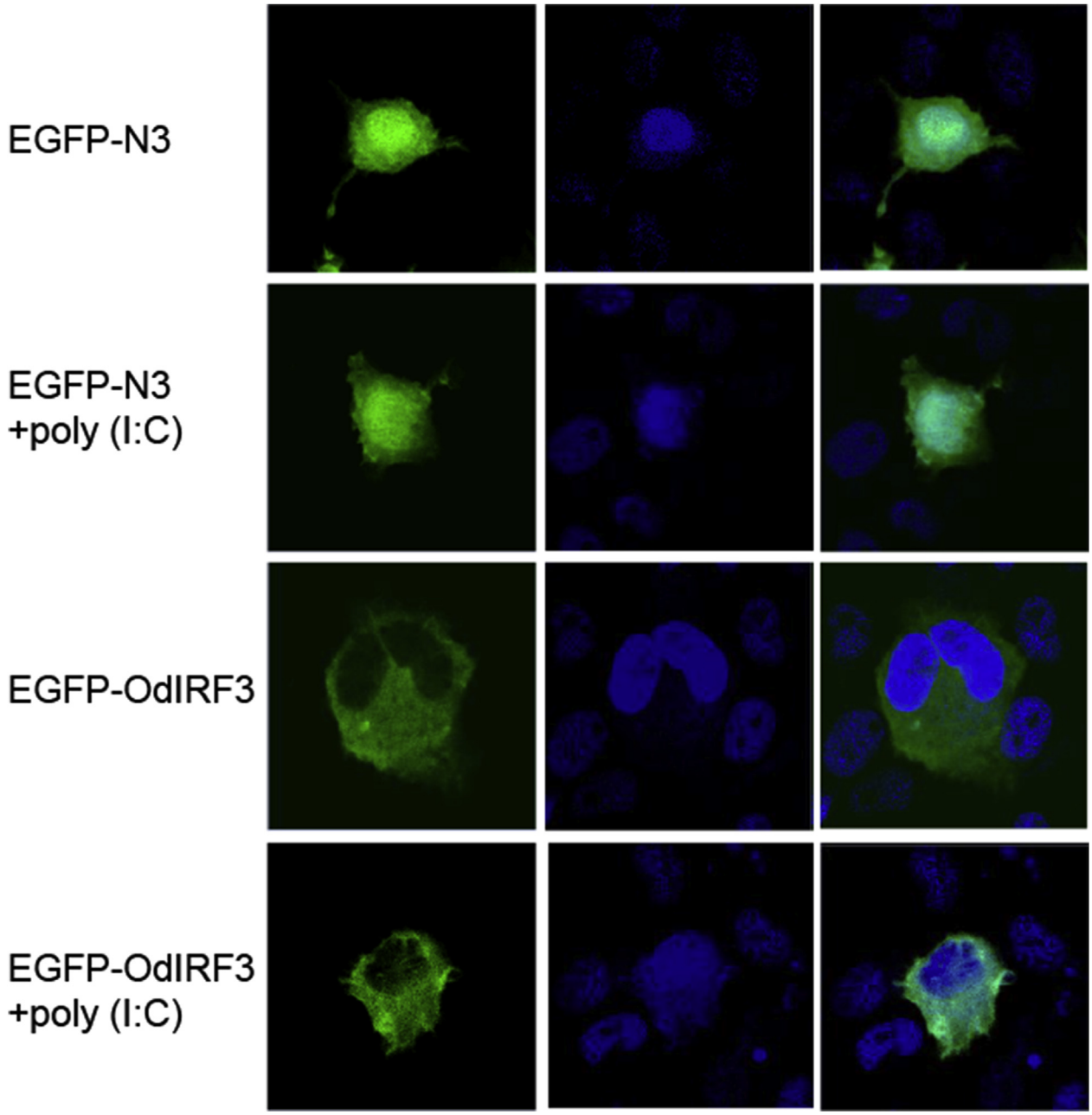

Fig. 5. Subcellular localization of OdIRF3. EPC cells seeded onto microscopy cover glass in 6-well plates were transfected with 2 μg EGFP-OdIRF3 or the empty vector. After 24 h, the cells were untreated (null) or transfected with 2 μg poly (I:C) for 12 h, then the cells were fixed and subjected to confocal microscopy analysis. Green staining represents the OdIRF3 protein signal, and blue staining indicates the nucleus region (original magnification, ×63; oil immersion objective). Bar, 10 μm. All experiments were repeated at least three times, with similar results. (For interpretation of the references to colour in this figure legend, the reader is referred to the Web version of this article.)

activation are different. This is consistent with the effect of crucian carp and zebrafish IRF3 on IFNφ3 regulation. In addition, four zebrafish type I IFNs (IFNφ1-4) have been identified, IFNφ1 and IFNφ4 bound to the same receptors complex, whereas IFNφ2 and IFNφ3 are recognized by a different one, therefore, their activators may be different [29]. Current research indicates that IRF7 can induce the expression of both DrIFNφ1 and DrIFNφ3; IRF3 and IRF7 may perform their biological functions through different signaling pathways [14].

In our study, OdIRF3 was located in the cytoplasm; upon stimulation with poly-I:C, nuclear aggregation of OdIRF3 occurred in some cells. This is distinguished from the IRF3 in mammals, in which IRF3 is unavailable without virus stimulation. Fish IRF3 could activate IFNpro without poly-I:C stimulation or viral infection, indicating that IRF3 function might be different in lower and higher vertebrates. The exact mechanism should be further clarified.

Further research indicated that OdIRF3 up-regulates the expression of *epcifn* and *epcmavs*, and there was no significant increase in *epcvig1*. The sequence of the vig1 promoter region has not been acquired, so we speculated that the ISRE is absent in fish vig1, or the function of fish vig1 is different from its antiviral role in mammals. Functionally, IRF3 play a vital role in antiviral response [30]. Our study demonstrated that SVCV replication was inhibited by ectopic expression of OdIRF3 significantly, similar with the findings in *Lateolabrax japonicas* and *Squaliobarbus curriculus* [31,32]. Thus, OdIRF3 exerted antiviral function against viral infection conservatively. Taken together, our study characterised OdIRF3 as a conserved IRF member according to the amino

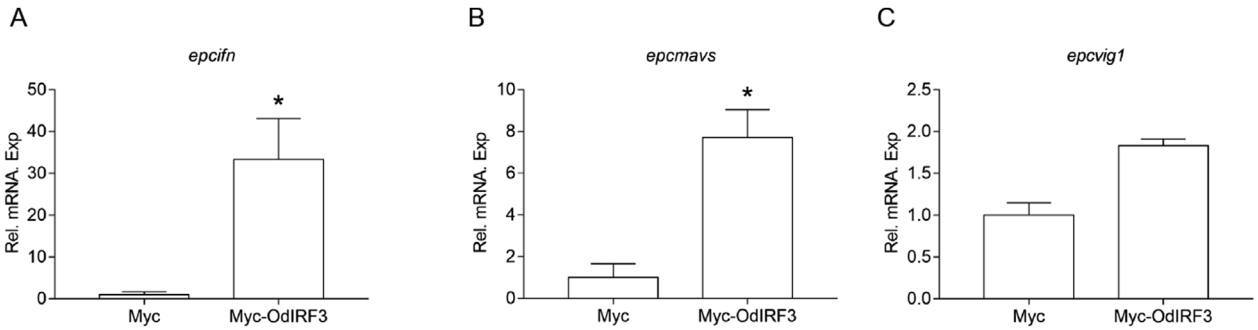

Fig. 6. Overexpression of OdIRF3 induces the expressions of ISGs in EPC cells. EPC cells were seeded in 6-well plates overnight and transfected with 1.5 μg OdIRF3-Myc or empty vector for 24 h. Then total RNAs were extracted to examine the transcripts of ifn (A), mavs (B), and vig1 (C) by qPCR. *β-actin* was used to normalise gene expression in each sample and expression is represented as fold change relative to the expression level in control cells. Error bars represents the means ± SEM (n = 3), and the experiments were repeated three time with similar results. Asterisks indicate significant differences from control (*$p < 0.05$).

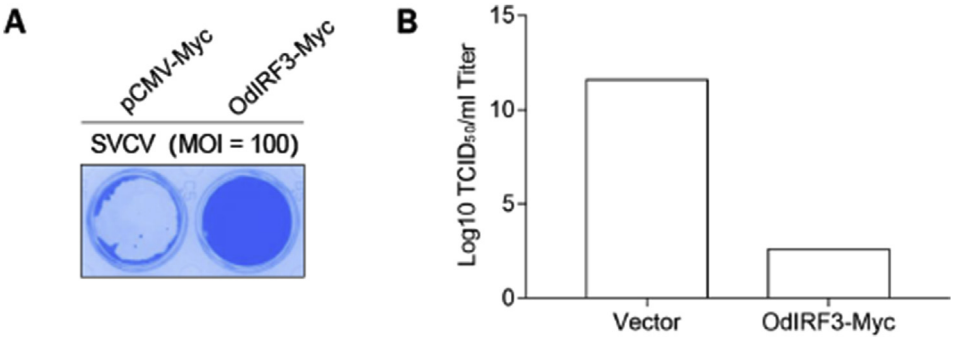

Fig. 7. OdIRF3 is a strong antiviral protein. (A and B) EPC cells seeded in 24-well plates overnight were transfected with 0.5 μg OdIRF3 or empty vector. At 24 h posttransfection, EPC cells were infected with SVCV (MOI = 100) per well for 48 h at 28 °C. (A) Then, cells were fixed with 4% PFA and stained with 1% crystal violet. (B) Culture supernatants from the cells infected with SVCV were collected, and the viral titer was measured by plaque assay. The experiments were performed for three times with similar results. (For interpretation of the references to colour in this figure legend, the reader is referred to the Web version of this article.)

acid sequence, IFN regulatory function, and antiviral capacity.

Conflicts of interest

The authors have no conflicting commercial or financial interest in publishing this paper.

Acknowledgments

We thank Dr. Fang Zhou (Institute of Hydrobiology, Chinese Academy of Sciences) for assistance with confocal microscopy analysis and Dr. Feng Xiong (China Zebrafish Resource Center, Institute of Hydrobiology, Chinese Academy of Sciences) for RNA sample extraction. This work was supported National Natural Science Foundation of China provided funding to Shun Li under grant number 31502200.

References

[1] A.M. Bruns, C.M. Horvath, LGP2 synergy with MDA5 in RLR-mediated RNA recognition and antiviral signaling, Cytokine 74 (2015) 198–206.
[2] M. Yoneyama, K. Onomoto, M. Jogi, T. Akaboshi, T. Fujita, Viral RNA detection by RIG-I-like receptors, Curr. Opin. Immunol. 32 (2015) 48–53.
[3] Z.A. Laghari, L. Li, S.N. Chen, H.J. Huo, B. Huang, Y. Zhou, et al., Composition and transcription of all interferon regulatory factors (IRFs), IRF1-11 in a perciform fish, the Mandarin fish, Siniperca chuatsi, Dev. Comp. Immunol. 81 (2018) 127–140.
[4] H. Feng, Y.B. Zhang, Q.M. Zhang, Z. Li, Q.Y. Zhang, J.F. Gui, Zebrafish IRF1 regulates IFN antiviral response through binding to IFN phi 1 and IFN phi 3 promoters downstream of MyD88 signaling, J. Immunol. 194 (2015) 1225–1238.
[5] M.H. Gu, G. Lin, Q.N. Lai, B. Zhong, Y. Liu, Y.C. Mi, et al., Ctenopharyngodon idella IRF2 plays an antagonistic transcriptional regulation of IFN and ISG genes, Dev. Comp. Immunol. 49 (2015) 103–112.
[6] S. Li, L.F. Lu, Z.X. Wang, D.D. Chen, Y.A. Zhang, Fish IRF6 is a positive regulator of IFN expression and involved in both of the MyD88 and TBK1 pathways, Fish Shellfish Immunol. 57 (2016) 262–268.
[7] X. Zhao, R.H. Wang, Y.G. Li, T.Y. Xiao, Molecular cloning and functional characterization of interferon regulatory factor 7 of the barbel chub, Squaliobarbus curriculus, Fish Shellfish Immunol. 69 (2017) 185–194.
[8] J. Shi, Y.B. Zhang, J.S. Zhang, J.F. Gui, Expression regulation of zebrafish interferon regulatory factor 9 by promoter analysis, Dev. Comp. Immunol. 41 (2013) 534–543.
[9] S. Li, L.F. Lu, H. Feng, N. Wu, D.D. Chen, Y.B. Zhang, et al., IFN regulatory factor 10 is a negative regulator of the IFN responses in fish, J. Immunol. 193 (2014) 1100–1109.
[10] K.A. Fitzgerald, S.M. McWhirter, K.L. Faia, D.C. Rowe, E. Latz, D.T. Golenbock, et al., IKK epsilon and TBK1 are essential components of the IRF3 signaling pathway, Nat. Immunol. 4 (2003) 491–496.
[11] X. Chen, Y. Shen, M. Wu, J. Zhao, Irf3 from Mandarin fish thymus initiates interferon transcription, Fish Physiol. Biochem. 45 (2019) 133–144.
[12] F. Sun, Y.B. Zhang, T.K. Liu, L. Gan, F.F. Yu, Y. Liu, et al., Characterization of fish IRF3 as an IFN-inducible protein reveals evolving regulation of IFN response in vertebrates, J. Immunol. 185 (2010) 7573–7582.
[13] R.H. Wang, Y.G. Li, Z.Y. Zhou, Q.L. Liu, L.B. Zeng, T.Y. Xiao, Involvement of interferon regulatory factor 3 from the barbel chub Squaliobarbus curriculus in the immune response against grass carp reovirus, Gene 648 (2018) 5–11.
[14] H. Feng, Q.M. Zhang, Y.B. Zhang, Z. Li, J. Zhang, Y.W. Xiong, et al., Zebrafish IRF1, IRF3, and IRF7 differentially regulate IFNPhi1 and IFNPhi3 expression through assembly of Homo- or heteroprotein complexes, J. Immunol. 197 (2016) 1893–1904.
[15] Q.Y. Zhang, H.M. Ruan, Z.Q. Li, X.P. Yuan, H.F. Gui, Infection and propagation of lymphocystis virus isolated from the cultured flounder Paralichthys olivaceus in grass carp cell lines, Dis. Aquat. Org. 57 (2003) 27–34.
[16] L.F. Lu, S. Li, X.B. Lu, S.E. LaPatra, N. Zhang, X.J. Zhang, et al., Spring viremia of carp virus N protein suppresses fish IFNphi1 production by targeting the mitochondrial antiviral signaling protein, J. Immunol. 196 (2016) 3744–3753.
[17] K.J. Livak, T.D. Schmittgen, Analysis of relative gene expression data using real-time quantitative PCR and the 2(T)(-Delta Delta C) method, Methods 25 (2001) 402–408.
[18] K.E. Luker, C.M. Pica, R.D. Schreiber, D. Piwnica-Worms, Overexpression of IRF9 confers resistance to antimicrotubule agents in breast cancer cells, Cancer Res. 61 (2001) 6540–6547.
[19] M. Huber, T. Suprunenko, T. Ashhurst, F. Marbach, H. Raifer, S. Wolff, et al., IRF9 prevents CD8(+) T cell exhaustion in an extrinsic manner during acute lymphocytic choriomeningitis virus infection, J. Virol. 91 (2017).
[20] K. Ozato, P. Tailor, T. Kubota, The interferon regulatory factor family in host defense: mechanism of action, J. Biol. Chem. 282 (2007) 20065–20069.
[21] K. Honda, T. Taniguchi, IRFs: master regulators of signalling by Toll-like receptors and cytosolic pattern-recognition receptors, Nat. Rev. Immunol. 6 (2006) 644–658.
[22] T. Mizutani, K. Tsuji, Y. Ebihara, S. Taki, Y. Ohba, T. Taniguchi, et al., Homeostatic erythropoiesis by the transcription factor IRF2 through attenuation of type I interferon signaling, Exp. Hematol. 36 (2008) 255–264.
[23] Y. Wang, D. Liu, P. Chen, H.P. Koeffler, X. Tong, D. Xie, Negative feedback regulation of IFN-gamma pathway by IFN regulatory factor 2 in esophageal cancers, Cancer Res. 68 (2008) 1136–1143.
[24] D. Xu, F. Meyer, E. Ehlers, L. Blasnitz, L. Zhang, Interferon regulatory factor 4 (IRF-4) targets IRF-5 to regulate Epstein-Barr virus transformation, J. Biol. Chem. 286

(2011) 18261–18267.
[25] C. Stein, M. Caccamo, G. Laird, M. Leptin, Conservation and divergence of gene families encoding components of innate immune response systems in zebrafish, Genome Biol. 8 (2007) R251.
[26] C. Shu, Q. Chu, D. Bi, Y. Wang, T. Xu, Identification and functional characterization of miiuy croaker IRF3 as an inducible protein involved regulation of IFN response, Fish Shellfish Immunol. 54 (2016) 499–506.
[27] A. Takahashi, Y. Kobayashi, K. Mizusawa, The pituitary-interrenal axis of fish: a review focusing on the lamprey and flounder, Gen. Comp. Endocrinol. 188 (2013) 54–59.
[28] G. Nardocci, C. Navarro, P.P. Cortes, M. Imarai, M. Montoya, B. Valenzuela, et al., Neuroendocrine mechanisms for immune system regulation during stress in fish, Fish Shellfish Immunol. 40 (2014) 531–538.
[29] D. Aggad, M. Mazel, P. Boudinot, K.E. Mogensen, O.J. Hamming, R. Hartmann, et al., The two groups of zebrafish virus-induced interferons signal via distinct receptors with specific and shared chains, J. Immunol. 183 (2009) 3924–3931.
[30] S.L. Schafer, R. Lin, P.A. Moore, J. Hiscott, P.M. Pitha, Regulation of type I interferon gene expression by interferon regulatory factor-3, J. Biol. Chem. 273 (1998) 2714–2720.
[31] W.W. Zhang, Z.L. Li, P. Jia, W. Liu, M.S. Yi, K.T. Jia, Interferon regulatory factor 3 from sea perch (Lateolabrax japonicus) exerts antiviral function against nervous necrosis virus infection, Dev. Comp. Immunol. 88 (2018) 200–205.
[32] R. Wang, Y. Li, Z. Zhou, Q. Liu, L. Zeng, T. Xiao, Involvement of interferon regulatory factor 3 from the barbel chub Squaliobarbus curriculus in the immune response against grass carp reovirus, Gene 648 (2018) 5–11.